Virtual permeametry on microtomographic images

by

Christoph H. Arns and Mark A. Knackstedt
Department of Applied Mathematics
Australian National University
Canberra ACT 0200 AUSTRALIA

W. Val Pinczewski
School of Petroleum Engineering
University of New South Wales
Sydney NSW 2052 AUSTRALIA

and

Nicos S. Martys
Building and Fire Research Laboratory
National Institute of Standards and Technology
Gaithersburg, MD 20899 USA

Reprinted from Journal of Petroleum Science and Engineering, Vol. 45, Issues 1-2, pp. 41-46, November 2004.

National Institute of Standards and Technology
Technology Administration, U.S. Department of Commerce

Available online at www.sciencedirect.com

SCIENCE DIRECT

Journal of Petroleum Science and Engineering 45 (2004) 41–46

Journal of Petroleum Science & Engineering

www.elsevier.com/locate/petrol

Virtual permeametry on microtomographic images

Christoph H. Arns[a,*], Mark A. Knackstedt[a], W. Val Pinczewski[b], Nicos S. Martys[c]

[a] *Department of Applied Mathematics, Res. School of Physical Sciences and Engineering, Australian National University, Canberra ACT 0200, Australia*

[b] *School of Petroleum Engineering, University of New South Wales, Sydney NSW 2052, Australia*

[c] *Materials and Construction Research Division, National Institute of Standards and Technology, Gaithersburg, MD 20899-8600, USA*

Abstract

We show that accurate numerical micropermeametry measurements can be performed on three-dimensional (3D) digitized images of sedimentary rock. The sample size can be very small, making it possible to predict properties from core material not suited for laboratory testing (e.g., drill cuttings, sidewall core and damaged core plugs). Simulation of fluid permeability on microtomographic images of Fontainebleau sandstone on sample sizes of less than 1 mm^3 are in good agreement with experimental measurements over a wide range of porosities.

Keywords: Porous media; X-ray-CT; Permeability; Fontainebleau

1. Introduction

The reliable prediction of the permeability of subsurface formations is of paramount importance to geophysicists, petroleum engineers and groundwater scientists. Permeability is commonly derived by empirical cross-property correlations based on logging measurements. Use of these relationships introduces considerable uncertainty in reservoir characterisation studies. A major source of the uncertainty is related to the present inability to effectively characterize complex rock microstructure at the pore scale. A significant reduction in the level of uncertainty requires the development of techniques to accurately characterize rock microstructure and to relate this information to measured flow properties. Research has been undertaken to develop realistic reconstructions of three-dimensional (3D) porous materials (Joshi, 1974; Adler et al., 1990, 1992; Hazlett, 1997; Yeong and Torquato, 1998). These methods have been very instructive in understanding general properties of complex media; however, direct prediction of permeability by Adler et al. (1990, 1992) and Hazlett (1997) from reconstructed samples have been only in fair agreement with experimental data. More recent reconstruction methods (Thovert et al., 2001; Arns et al., 2003) have led to good agreement for conductive transport properties. These methods have yet to be tested for permeability.

Direct measurement of a 3D structure is now readily available from synchotron and X-ray-computed microtomography (X-ray-μCT) (Dunsmuir et al., 1991; Spanne et al., 1994) and laser confocal micros-

* Corresponding author. Fax: +61-2-6125-0732.
E-mail address: christoph.arns@anu.edu.au (C.H. Arns).

0920-4105/$ - see front matter © 2004 Elsevier B.V. All rights reserved.
doi:10.1016/j.petrol.2004.05.001

copy (Fredrich et al., 1995). These techniques provide the opportunity to experimentally measure the complex morphology of the pore space of sedimentary rock in three dimensions, at resolutions down to a few micrometers. One can then replace synthetic images derived from statistical models with experimental data and base transport calculations directly on the measured three-dimensional microstructure. This has been done previously for fluid permeability of Fontainebleau sandstone by a number of groups (Spanne et al., 1994; Schwartz et al., 1994; Auzerias et al., 1996; Martys et al., 1999; Manwart et al., 2002). Due to limitations in computing resources and experimental constraints, the results of these studies have been limited in scope and inconclusive. First, the number of samples studied was limited by computational requirements. Second, due to limitations on μCT detector size and the natural heterogeneity of rock at small scales, it is difficult to make direct comparison with experiment; in all cases, the imaged microplugs exhibited a different porosity to the original core material on which experiments were performed. In the work of Spanne et al. (1994), the numerical calculation of permeability on five images of sizes 44^3 to 84^3 at 10-μm resolution exhibited broad variability and consistently underestimated the experimental data. Schwartz et al. (1994) and Auzerias et al. (1996) considered a 280^3 image of Fontainebleau sandstone at 7.5-μm resolution. Predictions of permeability were within ≈15% of experimental values. Martys et al. (1999) considered four large subsets of Fontainebleau (510^3, 5.7 μm per voxel) across a range of porosity and predictions were in agreement (≈15% to 40%) with the experiment. In the work of Manwart et al. (2002), calculations on a single 300^3, 7.5 μm per voxel data set was, after rescaling the permeability prediction to account for porosity variation, in reasonable agreement (≈30%) with the experiment. However, calculations on a single smaller subset 100^3 led to significant (>100%) errors.

Previously (Arns et al., 2001, 2002), we reported large-scale computational studies of the electrical conductivity and the elastic properties directly on microtomographic images. We showed that an extensive study incorporating careful simulation and minimization of several sources of numerical error allows one to derive accurate predictions of properties. The calculation of electrical conductivity (Arns et al., 2001) and elasticity (Arns et al., 2002) on digitized images of Fontainebleau sandstone at sample sizes down to (700 μm)^3 was in excellent agreement with experimental measurements over the full range of porosity. In this paper, we extend the computational study to the calculation of permeability. We find that although the fluctuations in the permeability are greater than that observed for the electrical conductivity and elasticity, one can still perform accurate numerical micropermeametry on 3D digitized images of sedimentary rock at these small scales. The results highlight the exciting potential to predict properties from core material not suited for laboratory testing including drill cuttings, sidewall core or damaged core.

2. Methodology

2.1. Image acquisition

The tomographic data used in this analysis are obtained from a suite of Fontainebleau sandstone. Fontainebleau sandstone provides the ideal experimental system for this study as a considerable amount of experimental data (Jacquin, 1964; Fredrich et al., 1993) is available. The images were obtained from 4.52-mm-diameter cylindrical core samples extracted from each of four blocks of Fontainebleau sandstone with bulk porosity $\phi = 7.5\%$, 13%, 15%, 22%. A 2.91-mm length of each core was imaged (Flannery et al., 1987; Dunsmuir et al., 1991; Spanne et al., 1994). The reconstructed images have a resolution of 5.7 μm resulting in $795 \times 795 \times 512$ imaged sections. Each grey-scale image was thresholded using a kriging-based thresholding method (Oh and Lindquist, 1999) to give a binary pore-solid image (Lindquist et al., 2000). From the original cylindrical plug, we extract a 480^3 cubic subset for analysis corresponding to a volume of (2.73 mm)^3.

2.2. Numerical simulation and error analysis

A microstructure defined by a digital image is already naturally discretized and lends itself immediately to numerical computation of any number of quantities. The permeability calculation is based on a lattice-Boltzmann method (LB) using D3Q19 (3 Dimensional lattice with 19 possible momenta components; Qian et al., 1986). The implementation of the algorithm is similar to that detailed by Martys et al. (1999). The physical boundary condition at solid–fluid interfaces is the no-flow condition which in the LB methods is most simply realised by the bounce-back rule (Martys and Chen, 1996). The pressure gradient acting on the fluid is simulated by a body force (Ferreol and Rothman, 1995). Mirror-image boundary conditions (Martys et al., 1999) are applied in the plane perpendicular to the flow direction and all simulations were performed on an $L \times L \times 2L$ system; permeability is measured in the central (L^3) subset. Diagonal links in the D3Q19 model allow the fluids to leak to neighbouring lattice points which have only a single edge in common which can lead to inaccurate results for systems near disconnection (Manwart et al., 2002). To eliminate diagonal links which cross a solid boundary, we implement an erosion/dilation step on the pore space (Serra, 1982). The step reduces the porosity ϕ of the original tomographic image by a very small fraction $\approx 0.04\%$ but ensures that no flow occurs across disconnected pores. In all cases, the LB relaxation parameter $\tau = 1.0$ is used.

Before reporting numerical results, we must ensure that numerical artefacts are minimised. First, we consider finite size effects; here we aim to ensure that the size of the image is large enough to give useful predictions. This requires comparison of grid size to some statistical length scale (e.g., correlation length, average grain size). Errors will occur if we use too few pores/grains in the system to calculate the numerical permeability. We wish to choose a system size, which has an acceptable finite size error, but is small enough to be computationally feasible. In Fig. 1(a), we compare data measured on the 3 higher porosity images at different scales; 8 subsets gener-

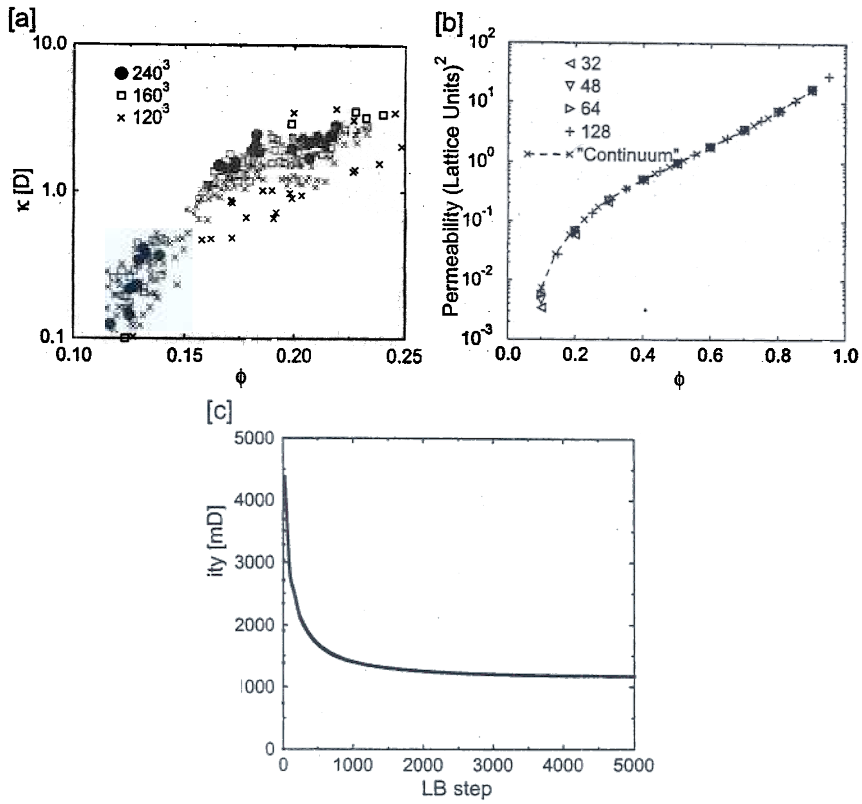

Fig. 1. (a) Results for numerical permeametry at 240^3 (●), 160^3 (□), and 120^3 (×) scales. This illustrates that finite size errors at 120^3 remain small. (b) No appreciable discretization error is noted for the permeability of a periodic array of spheres. (c) Evolution of the permeability solution with steps in the LB solver shows convergence.

ated at 240^3 to 27 subsets at 160^3 and 64 subsets at 120^3. The permeability measured on the smaller subsets is in good agreement with calculations on larger scales. While the variability observed in the smaller cells varies over a factor of three, this variability is not unlike the experimental scatter observed in classical porosity/permeability data. The ability to use small block sizes to estimate permeability is an exciting prospect. First, the permeability calculation is computationally feasible on a common workstation. Second, the combination of smaller image sizes on a large-imaged core, combined with the natural heterogeneity of rock, allow us to derive the permeability for the samples across a larger range ϕ. Finally, data sets at 120^3 (≈ 700 μm^3) are below the scale of drill cuttings.

Another potential numerical error, particularly when simulating permeability, is insufficient image resolution. This was originally discussed by Martys et al. (1999) who performed simulations on microtomographic images of Fontainebleau sandstone at a large scale (510^3). For low-porosity samples, the presence of small pores led to the conclusion that the resolution was not adequate to produce accurate flow fields. For this case, fine graining of the pore space by a factor of two was necessary to acquire sufficient resolution for realistic simulation.

It has been previously shown (Arns et al., 2001; Moctezuma-Berthier et al., 2002) that when simulating transport properties on voxelated data, a large (>30%) discretization error can be made. This error is due to the use of discrete voxels to represent continuum objects when simulating properties from microtomographic images. Errors due to discretization can include, for example, inaccurate description of curved grain boundaries and closing of narrow pores. To measure this effect, one should generate realisations of the original tomographic data sets at integer multiples of the resolution of the original image. Unfortunately, insufficient resolution in the coarse-grained digitized microstructures leads to poor numerical accuracy. To test for the importance of discretization on permeability, we consider the permeability of a model morphology, one based on periodic arrays of spheres varying across a range of porosities calculated at varying discretizations. The prediction in Fig. 1(b) shows that the errors in permeability due to discretization are minimal.

For the subsets at $\phi = 13\%$, 15%, 22%, we simulate the permeability on the 64 independent 120^3 subsets in three orthogonal directions. In Fig. 1(c), we show the evolution of the numerical solution for permeability over the number of iterations for a 120^3 subset. Relaxation to an asymptotic value for k is clearly observed within 5000 iterations and this cutoff is used in all simulations at this scale. The runtime on a 1-GHz Alpha processor for a single sample at porosity $\phi = 10\%$ is ≈ 80 processor min. The runtime increases linearly with porosity. Generation of the permeability on all subsets of the original images requires the equivalent of 2 processor months.

As discussed above, the image resolution for the low-porosity Fontainebleau samples $\phi = 7.5\%$ is insufficient (not enough voxels within a single pore) to produce a reliable flow field. To allow for accurate simulation, we fine grain the original 120^3 image; replace each voxel by a $2 \times 2 \times 2$ voxels of the same phase, thus giving a system at $240^2 \times 480$ at 2.85-μm voxel size. A total of 10,000 iterations are used as a cutoff at this scale. These simulations on the 64 independent subsets along three orthogonal directions required approximately 3 months of equivalent processor time to complete.

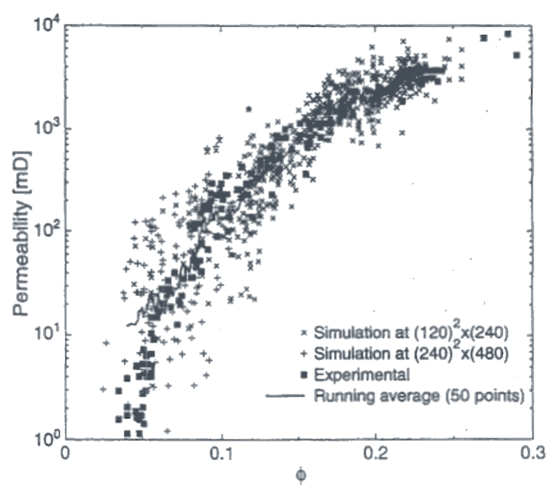

Fig. 2. Comparison of the numerical prediction of the permeability simulations for the Fontainebleau sandstone with experimental data. The lines indicate best fits to the numerical data.

3. Results

In Fig. 2, we compare the computed continuum permeability k of the Fontainebleau sandstone with experimentally measured values of Jacquin (1964) and Fredrich et al. (1993). The predicted k is in good agreement with the experimental data for all porosities and the variation in k is similar to that observed experimentally. Remarkably, the large number of simulated data points (>750) generated from subsets of four cores at a scale of $(2.7\ \mathrm{mm})^3$ encompass a broad range of porosity and allow one to generate a representative k:ϕ relationship across nearly four orders of magnitude in permeability. The scale of the four original cores $(2.7\ \mathrm{mm})^3$ is of the scale of large drill cuttings and illustrates the potential to predict permeability from core material which is not suited for laboratory testing.

4. Conclusion

We have shown that by estimating and minimizing several sources of numerical error, very accurate predictions of permeability can be derived directly from digitized microtomographic images at a small scale. The combination of appropriate choice of window sizes on the imaged core and the natural heterogeneity of the rock allowed us to derive permeability–porosity relationships across a range of porosity from four subsamples $[\simeq(2.7\ \mathrm{mm})^3]$. The utility of small sample sizes highlights a potential for predicting properties from core material not suited for laboratory testing (e.g., drill cuttings, sidewall core and damaged core plugs).

Tomographic imaging facilities now have the ability to image samples in 3D with unprecedented speed and imaging resolution. The combination of high-brilliance X-ray sources, fast high-resolution X-ray detector systems, high-speed data networks, and large-scale computation gives one the ability to virtually reconstruct 3D images in real time. Computational techniques and hardware have similarly progressed to the point where one can calculate properties on 3D voxelated images over short time scales. One can envision the routine calculation of the porosity–permeability relationship via numerical techniques on core material for a specific reservoir. The total computational time required to calculate the data points in Fig. 2 was $\simeq 150$ processor days, with moderate computational resources (e.g., a 64-node pc cluster) this permeability–porosity correlation could be generated in 60 h. Optimising the LB permeability solver or use of a finite difference code may further reduce the computational loads. The parallel development of these experimental and computational methods demonstrates the potential to develop a virtual core laboratory, a facility for the imaging and calculation of petrophysical properties on core material. This *virtual lab* has enhanced capabilities as one may obtain data from core material which to date have been considered unsuitable for testing. Moreover, numerical simulation offers the ability to measure local information (e.g., flow paths, tortuosity) on complex samples, information which to date is not experimentally realisable.

Acknowledgements

MAK and WVP thank the Australian Research Council, and MAK, the Australian Partnership for Advanced Computing (APAC) for financial support. NSM thanks the HYPERCON program at NIST for partial financial support. We thank APAC and the ANU Supercomputing Facility for very generous allocations of computer time.

References

Adler, P., Jacquin, C., Quiblier, J., 1990. Flow in simulated porous media. Int. J. Multiph. Flow 16, 691–712.

Adler, P., Jacquin, C., Thovert, J.-F., 1992. The formation factor of reconstructed porous media. Water Resour. Res. 28, 1571.

Arns, C.H., Knackstedt, M.A., Pinczewski, W.V., Lindquist, W.B., 2001. Accurate computation of transport properties from microtomographic images. Geophys. Res. Lett. 28, 3361–3364.

Arns, C.H., Knackstedt, M.A., Pinczewski, W.V., Garboczi, E.G., 2002. Computation of linear elastic properties from microtomographic images: methodology and agreement between theory and experiment. Geophysics 67, 1396–1405.

Arns, C.H., Knackstedt, M.A., Mecke, K.R., 2003. Reconstructing complex materials via effective grain shapes. Phys. Rev. Lett. 91 (215506), 1–4.

Auzerias, F.M., Dunsmuir, J., Ferreol, B.B., Martys, N., Olson, J., Ramakrishnan, T.S., Rothman, D.H., Schwartz, L.M., 1996. Transport in sandstone: a study based on three dimensional microtomography. Geophys. Res. Lett. 23, 705–708.

Dunsmuir, J.H., Ferguson, S.R., D'Amico, K.L., 1991. Design and operation of an imaging X-ray detector for microtomography. IOP Conf. Ser. 121, 257–261.

Ferreol, B., Rothman, D., 1995. Lattice-Boltzmann simulations of flow through Fontainebleau sandstone. Transp. Porous Media 20, 3–20.

Flannery, B.P., Deckman, H.W., Roberge, W.G., D'Amico, K.L., 1987. Three-dimensional X-ray microtomography. Science 237, 1439–1444.

Fredrich, J., Greaves, K., Martin, J., 1993. Pore geometry and transport properties of Fontainebleau sandstone. Int. J. Rock Mech. Min. Sci. 30, 691–697.

Fredrich, J., Menendez, B., Wong, T.F., 1995. Imaging the pore structure of geomaterials. Science 268, 276–279.

Hazlett, R.D., 1997. Statistical characterization and stochastic modeling of pore networks in relation to fluid flow. Math. Geol. 29, 801–821.

Jacquin, C.G., 1964. Corrélation entre la perméabilité et les caractéristiques géométriques du grès de Fontainebleau. Rev. Inst. Fr. Pet. 19, 921.

Joshi, M., 1974. A class of stochastic models for porous materials. PhD thesis, University of Kansas, Lawrence.

Lindquist, W.B., Venkatarangan, A., Dunsmuir, J., Wong, T.F., 2000. Pore and throat size distributions measured from synchrotron X-ray tomographic images of Fontainebleau sandstones. J. Geophys. Res. 105B, 21508.

Manwart, C., Aaltosalmi, U., Koponen, A., Hilfer, R., Timonen, J., 2002. Lattice-Boltzmann and finite-difference simulations for the permeability for three-dimensional porous media. Phys. Rev., E 66, 016702.

Martys, N.S., Chen, H., 1996. Simulation of multicomponent fluids in complex three-dimensional geometries by the lattice Boltzmann method. Phys. Rev., E 53, 743–750.

Martys, N.S., Hagedorn, J.G., Goujon, D., Devaney, J.E., 1999. Large scale simulations of single and multi component flow in porous media. SPIE 309, 403.

Moctezuma-Berthier, A., Vizika, O., Adler, P.M., 2002. Macroscopic conductivity of vugular porous media. Transp. Porous Media 49, 331–332.

Oh, W., Lindquist, W.B., 1999. Image thresholding by indicator kriging. IEEE Trans. Pattern Anal. Mach. Intell. 21, 590.

Qian, Y.H., d'Humieres, D., Lamelland, P., 1986. Lattice BGK models for Navier-stokes equation. Europhys. Lett. 2, 291.

Schwartz, L.M., Auzerias, F.M., Dunsmuir, J., Martys, N., Bentz, D.P., Torquato, S., 1994. Transport and diffusion in three-dimensional composite media. Physica, A 207, 28–36.

Serra, J., 1982. Image Analysis and Mathematical Morphology. Academic Press, Amsterdam.

Spanne, P., Thovert, J., Jacquin, J., Lindquist, W.B., Jones, K., Adler, P.M., 1994. Synchotron computed microtomography of porous media: topology and transports. Phys. Rev. Lett. 73, 2001–2004.

Thovert, J.-F., Yousefian, F., Spanne, P., Jacquin, C.G., Adler, P.M., 2001. Grain reconstruction of porous media: application to a low-porosity Fontainebleau sandstone. Phys. Rev., E 63, 61307.

Yeong, C.L.Y., Torquato, S., 1998. Reconstructing random media. Phys. Rev., E 57, 495.